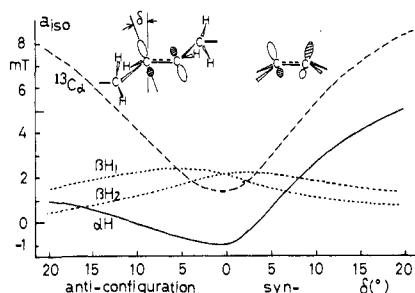


**Table I.** Proton Hyperfine Couplings Observed for the Anion and Cation Radicals of Hexene Isomers in *n*-Hexane Matrices

molecule		coupling (mT)	
		anion	cation
<i>trans</i> -3-hexene (in C <sub>6</sub> D <sub>14</sub> )	$\alpha\text{H} \times 2$	$ 0.5, 0.1, -0.3  \pm 0.1$	1.3
	$\beta\text{H} \times 2$	1.38	4.6
	$\beta\text{H} \times 2$	0.56	2.9
<i>trans</i> -2-hexene (in C <sub>6</sub> H <sub>14</sub> )	$\alpha\text{H} \times 2$	$ 0.7, 0.2, -0.3  \pm 0.2$	1.3
	$\beta\text{H} \times 2^a$	1.45	3.9
	$\beta\text{H} \times 2^a$	0.9	3.9
1-hexene (in C <sub>6</sub> H <sub>14</sub> )	$\alpha\text{H} \times 2$	$ 0.7, 0.2, -0.3  \pm 0.2$	-
	$\alpha\text{H} \times 1$	$ 1.3, 0.7, 0.1 $	-
	$\beta\text{H} \times 1$	1.6	-
	$\beta\text{H} \times 1$	0.8	-

<sup>a</sup>The methyl rotation is frozen at 4.2 K. The third  $\beta$ -proton coupling of the methyl group was not resolved and is estimated to be less than 0.2 mT from the ESR line widths.

**Figure 2.** The proton hyperfine couplings for the *trans*-3-hexene radical anion obtained by INDO molecular orbital calculation (see text).

could be reproduced only by a pair of hyperfine coupling tensors of equivalent  $\alpha$ -protons ( $|A|(H_\alpha \times 2) = |(0.5, 0.1, -0.3)| \pm 0.1$  mT) and two pairs of isotropic couplings of equivalent  $\beta$ -protons ( $a(H_{\beta 1} \times 2) = 1.38$  mT,  $a(H_{\beta 2} \times 2) = 0.56$  mT; Table I). The three pairs of equivalent proton couplings obtained indicate that the radical has a C<sub>2</sub> symmetry of the parent molecules ( $-\text{CH}_2\text{CH}=\text{CHCH}_2-$ ). The dipolar tensors of the two  $\alpha$ -protons are not small ( $B = 0.4, 0, -0.4$  mT), suggesting that each half of the unpaired electron spin density resides on the equivalent C=C  $\alpha$ -carbon atoms. The small isotropic couplings for  $\beta$ - and  $\alpha$ -protons cannot be explained by alkyl, allyl, or vinyl radicals or planar  $\pi$  ion radicals. The small  $\alpha$ -proton couplings ( $a(H_\alpha) = \pm 0.1$  mT) suggest that the species has a pyramidal radical structure with a  $\sigma$ -character.  $\sigma$ -type radicals are known to have small  $\alpha$ -proton couplings by cancelling the contributions of spin polarization and spin delocalization.<sup>11</sup> The irradiation of the mixed crystals of hexane containing 1- or *trans*-2-hexene yielded also the corresponding alkene anions with similar pyramidal radical structures. The preliminary results obtained are listed in Table I.

The pyramidal structure in the anti configuration of alkene anions was supported by INDO MO calculations, which results are shown in Figure 2. The MO calculations gave proton hyperfine couplings agreeable with the observed values in the case of the anti configuration of a pyramidal radical structure with a 10–15° deviation from the plane. The minimum of the total energy was also obtained in the anti configuration, although the angle of the nonplanarity is small ( $\sim 3^\circ$ ). On the other hand, the MO calculations for the syn conformation and for the twist radical structure did not result in small  $\alpha$ -proton and  $\beta$ -proton couplings, respectively, excluding the occurrence of their forms.<sup>10</sup>

Alkene radical cations ( $\text{RCH}=\text{CHR}^{+\bullet}$ ) have been reported to have a planar structure except for vinyl derivatives ( $\text{CH}_2=\text{CR}_1\text{R}_2$ ) with a twisted structure and to be stabilized by hyperconjugation to the CH  $\beta$ -bonds and/or CH  $\alpha$ -bonds,<sup>5–7</sup> while the anions may be stabilized by mixing  $[2s;C]$  atomic orbital with a larger core integral to the  $[2p;C]$  orbitals, resulting in a pyramidal radical structure.

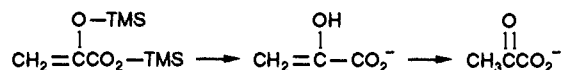
(11) Fessenden, R. W.; Schuler, R. H. *J. Chem. Phys.* **1963**, *39*, 2147.**Preparation and Properties of Enolpyruvate**James A. Peliska<sup>†</sup> and Marion H. O'Leary\*Departments of Chemistry and Biochemistry  
University of Wisconsin, Madison, Wisconsin 53706

Received October 9, 1990

The enolic form of pyruvate is considered to be a key intermediate in enzymatic reactions catalyzed by pyruvate kinase, phosphoenolpyruvate carboxylase, pyruvate-phosphate dikinase, malic enzyme, and oxalacetate decarboxylase,<sup>1</sup> but few direct studies have examined the reactions or kinetic competency of enolpyruvate.<sup>2</sup> Enolpyruvate has been formed by the action of acid phosphatase on phosphoenolpyruvate in acidic solutions<sup>3–6</sup> and found to have reasonable kinetic stability in D<sub>2</sub>O at low buffer concentrations ( $t_{1/2} = 3.6$  min at 20 °C in D<sub>2</sub>O, pD = 6.4). However, this method is not ideal for detailed study of enolpyruvate because the solution necessarily contains protein, phosphoenolpyruvate, phosphate, buffer, and other undesirable materials, and only a limited range of pH is accessible. In this paper we present a simple, clean, and effective method for generating and studying enolpyruvate that is free of these limitations. The material thus generated has the expected kinetic properties and permits direct estimation of the rate of water-catalyzed ketonization of enolpyruvate.

We synthesized bis-TMS-enolpyruvate (i.e., 2-((trimethylsilyloxy)propenoic acid trimethylsilyl ester), in 51% yield by the deprotonation of pyruvic acid with triethylamine and silylation with trimethylsilyl chloride in dimethylformamide.<sup>7</sup> The compound showed the expected NMR, IR, and mass spectra and was stable for several weeks at –20 °C.

When bis-TMS-enolpyruvate was injected directly into buffer solutions in D<sub>2</sub>O (final concentration 0.5 mM) and the time-dependent change in the absorbance at 225 nm recorded, biphasic kinetics were observed, showing an initial rapid absorbance increase followed by a slower decrease, presumably because of relatively rapid hydrolysis of the two TMS groups, followed by slow ketonization. Similar biphasic kinetics have been reported for the hydrolysis and tautomerization of vinyl acetals.<sup>8</sup>



When fluoride was used to effect cleavage of the TMS groups, the initial phase was eliminated, presumably because cleavage of the TMS groups became fast.<sup>9</sup> The absorbance change observed then followed clean first-order kinetics, with a rate constant essentially the same as that of the second phase observed above. In the absence of added buffer, the ketonization half-life at 20 °C was estimated to be about 7 min in D<sub>2</sub>O. As originally ob-

\* Present address: Department of Biochemistry, University of Nebraska, Lincoln, NE 68583.

† Present address: Department of Chemistry, The Pennsylvania State University, University Park, PA 16802.

(1) O'Leary, M. H. *The Enzymes* (3rd Ed.), in press.(2) Rose, I. A. *Methods. Enzymol.* **1982**, *87*, 84.(3) Kuo, D. J.; Rose, I. A. *J. Am. Chem. Soc.* **1978**, *100*, 6289.(4) Kuo, D. J.; O'Connell, E. L.; Rose, I. A. *J. Am. Chem. Soc.* **1979**, *101*, 5025.(5) Kuo, D. J.; Rose, I. A. *J. Am. Chem. Soc.* **1982**, *104*, 3235.(6) Miller, B. A.; Leussing, D. L. *J. Am. Chem. Soc.* **1985**, *107*, 7146.(7) House, H. O.; Czuba, L. J.; Gall, M.; Olmstead, H. D. *J. Org. Chem.* **1969**, *34*, 2324. To a solution of pyruvic acid (4.0 g) in 30 mL of DMF was added 14.0 g of triethylamine, followed by 15.0 g of TMSCl. Triethylammonium chloride precipitated immediately. After stirring at room temperature for 2 h, the supernatant solution was extracted with hexane. Evaporation of the hexane yielded 5.4 g (51%) of bis(trimethylsilyl)enolpyruvate. NMR, IR, and mass spectra were consistent with the assigned structure. This material was stored at –30 °C as an ether solution, which was used directly in further experiments.(8) Chiang, Y.; Chwang, W. K.; Kresge, A. J.; Yin, Y. *J. Am. Chem. Soc.* **1989**, *111*, 7185.(9) Approximately 0.5  $\mu\text{L}$  of TMS-enolpyruvate, neat or as an ether solution, was injected into 10  $\mu\text{L}$  of D<sub>2</sub>O containing 200 mM tetrabutylammonium fluoride and mixed vigorously. After 45 s this solution was injected into the equilibrated buffer solution by using a mixing foot, and the change in absorbance at 225 nm was recorded. Final concentrations of enol in the reaction mixtures were typically 0.4–0.5 mM.

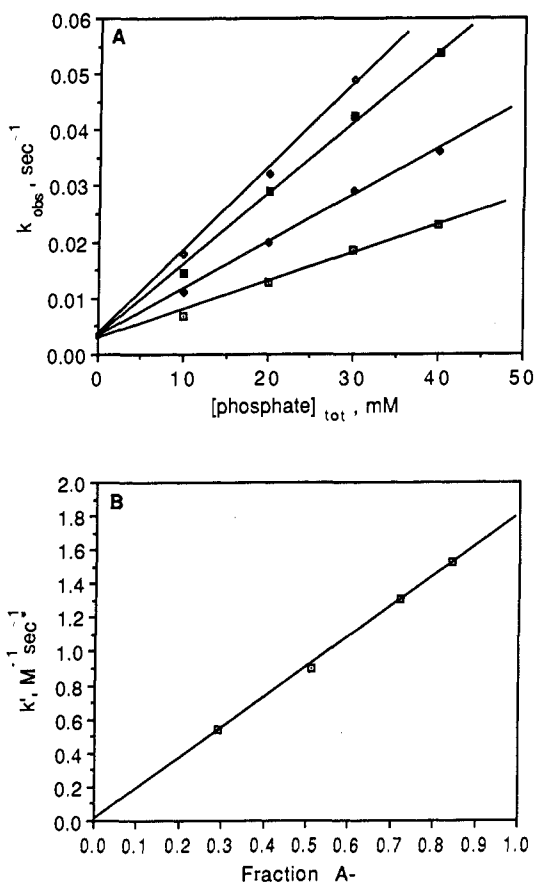


**Figure 1.** (A) Plot of the observed first-order rate constants vs total buffer concentration for the ketonization of enolpyruvate at various fixed pH levels at 20 °C. Reactions were run in the presence of 10–40 mM phosphate buffer at the following fixed pH levels: 7.0 (□), 7.4 (◇), 7.8 (■), and 8.1 (◆). Ionic strength was maintained at 0.1 by the addition of KCl. (B) The dependence of  $k'$  ( $k_{\text{obs}} - k_0 / [\text{phosphate}]$ ) on the mole fraction of the general base  $\text{DPO}_3^{2-}$ .

served by Rose et al., ketonization is severalfold faster in  $\text{H}_2\text{O}$  than in  $\text{D}_2\text{O}$ .<sup>10</sup> This same method of generating enols in aqueous buffer solutions has previously been used to study ketonization of monofunctional enols.<sup>11</sup>

When TMS-enolpyruvate was dissolved in  $d_3$ -acetonitrile, the NMR spectrum showed doublets for two nonequivalent vinyl protons at 5.50 and 4.93 ppm ( $J = 0.87$  Hz), along with TMS peaks at 0.2 and 0.3 ppm. Low-intensity doublets at 4.83 and 5.10 ppm, presumably from a small amount of TMS-enolpyruvic acid, were also observed. Upon addition of a small amount of  $\text{D}_2\text{O}$ , the two vinyl signals were rapidly replaced by doublets at 4.77 and 5.06 ppm ( $J = 1.26$  Hz). These signals then decayed over several minutes with concomitant increase of a triplet at 2.35 ppm corresponding to monodeuterated pyruvate. This suggests that both the TMS ester and TMS ether cleavage reactions are fast and the ketonization step is rate-determining. Similar results were observed in pure  $\text{D}_2\text{O}$  solvent.

The rates of the ketonization of enolpyruvate were studied in phosphate buffers in  $\text{D}_2\text{O}$  over a pH range of 7.0–8.1 (Figure 1). Least-squares analysis of these data gave a good fit with a pH-independent intercept rate constant of  $2.0 \pm 0.1 \times 10^{-3} \text{ s}^{-1}$  and a zero intercept in the replot at zero  $\text{H}_2\text{PO}_4^-$  concentration, indicating that only general base catalysis or the kinetically indistinguishable specific base–general acid catalysis operates.<sup>12</sup> The

(10) The rate difference between reactions in  $\text{H}_2\text{O}$  and in  $\text{D}_2\text{O}$  depends on the assumption made about effects of  $\text{D}_2\text{O}$  on buffer  $\text{p}K_a$  values. Our experience suggests that, at the same concentration of buffer, the solvent isotope effect is about 3.

(11) Chiang, Y.; Kresge, A. J.; Walsh, P. A. *J. Am. Chem. Soc.* **1986**, *108*, 6314.

(12) Jencks, W. P. *Catalysis in Chemistry and Enzymology*; McGraw-Hill: New York, 1969; pp 163–242.

apparent general base rate constant is  $1.81 \pm 0.05 \text{ M}^{-1} \text{ s}^{-1}$  at 20 °C. Analysis of the data by the method of Kresge<sup>8,13</sup> reveals that the reaction proceeds entirely through the enolate and thus follows the specific base–general acid mechanism. If the  $\text{p}K_a$  of enolpyruvate is assumed<sup>6</sup> to be 12, the bimolecular rate constant for protonation of the enolate by  $\text{H}_2\text{PO}_4^-$  ion is  $8 \times 10^4 \text{ M}^{-1} \text{ s}^{-1}$ .

Enolpyruvate is generated efficiently and quickly by the method described here. The enol undergoes buffer-catalyzed ketonization to give pyruvate in a manner consistent with that of a variety of other enols. The data presented here suggest that enolpyruvate is sufficiently stable in solutions of low buffer content ( $t_{1/2} = 1.8$  min in 10 mM phosphate buffer, pH 7.0, 20 °C or 7 min at zero buffer concentration) to allow studies of its intermediary role in enzyme-catalyzed reactions.

(13) Kresge, A. J. *Chem.-Tech. (Heidelberg)* **1986**, *16*, 250.

### Multiphasic Intracomplex Electron Transfer from Cytochrome *c* to Zn Cytochrome *c* Peroxidase: Conformational Control of Reactivity

Sten A. Wallin,<sup>1a</sup> Eric D. A. Stemp,<sup>1a</sup> Andrew M. Everest,<sup>1a</sup> Judith M. Nocek,<sup>1a</sup> Thomas L. Netzel,<sup>\*1b,c</sup> and Brian M. Hoffman<sup>\*1a</sup>

*Department of Chemistry, Northwestern University  
Evanston, Illinois 60208  
Amoco Technology Company, Naperville, Illinois 60566  
Received June 14, 1990*

We have shown recently that the photoinitiated  ${}^3(\text{MP}) \rightarrow \text{Fe}^{3+}\text{P}$  ( $\text{P} = \text{porphyrin}$ ;  $\text{M} = \text{Zn, Mg}$ ) and subsequent thermal  $\text{Fe}^{2+}\text{P} \rightarrow (\text{MP})^+$  electron transfer (ET) process within mixed-metal hemoglobin hybrids can be described by a kinetic mechanism suitable for a conformationally rigid system, Scheme I.<sup>2</sup> Our early data for the same ET processes within  $[\text{ZnCcP,Cc}]$  complexes ( $\text{ZnCcP} = \text{zinc-substituted cytochrome } c \text{ peroxidase}$ ,  $\text{Cc} = \text{cytochrome } c$ ) also was interpreted with Scheme I.<sup>3</sup> However, data obtained with improved signal/noise now shows that the  $\text{I} \rightarrow \text{A}$  process in  $[\text{ZnCcP,Cc}]$  cannot be described by this simple scheme and indicates that the electron-transfer intermediate,  $[(\text{ZnP})^+\text{CcP,Fe}^{2+}\text{P}]$  (I), exists in multiple bound forms that exhibit remarkably different rate constants for the  $\text{Fe}^{2+}\text{P} \rightarrow (\text{ZnP})^+$  ET reaction.

The triplet state,  $\text{A}^*$ , of the  $[\text{ZnCcP,Fe}^{3+}\text{Cc}]$  complex decays exponentially when excess  $\text{Fe}^{3+}\text{Cc}$  is present.<sup>4</sup> Scheme I for a rigid complex then predicts that I appears with the larger of the triplet decay and thermal ET rate constants,  $k_p$  and  $k_b$ , respectively, and disappears with the smaller according to the equation

$$[I(t)] = [A^*(0)]k_t \frac{\{e^{-k_p t} - e^{-k_b t}\}}{k_b - k_p} \quad (1)$$

In our original examination of  $[\text{ZnCcP,Cc}]$  complexes, we detected a slowly decaying kinetic transient for I when using a vertebrate Cc (tuna),  $k_b \sim 30 \text{ s}^{-1} < k_p$ , but a rapidly appearing transient with a fungal Cc (yeast iso-1),  $k_b \sim 10^4 \text{ s}^{-1} > k_p$ .<sup>3</sup> High-sensitivity

(1) (a) Northwestern University. (b) Amoco Technology Company. (c) Present Address: Department of Chemistry, Georgia State University, Atlanta, GA 30303.

(2) (a) Natan, M. J.; Hoffman, B. M. *J. Am. Chem. Soc.* **1989**, *111*, 6468–6470. (b) Natan, M. J.; Kuila, D.; Baxter, W. W.; King, B. C.; Hawkrige, F. M.; Hoffman, B. M. *J. Am. Chem. Soc.* **1990**, *112*, 4081–4082.

(3) (a) Ho, P. S.; Sutoris, C.; Liang, N.; Margoliash, E.; Hoffman, B. M. *J. Am. Chem. Soc.* **1985**, *107*, 1070–1071. (b) Liang, N.; Kang, C. H.; Ho, P. S.; Margoliash, E.; Hoffman, B. M. *J. Am. Chem. Soc.* **1986**, *108*, 4665–4666. (c) Liang, N.; Pielak, G. J.; Mauk, A. G.; Smith, M.; Hoffman, B. M. *Proc. Natl. Acad. Sci. U.S.A.* **1987**, *84*, 1249–1252. (d) Liang, N.; Mauk, A. G.; Pielak, G. J.; Johnson, J. A.; Smith, M.; Hoffman, B. M. *Science (Washington, D.C.)* **1988**, *240*, 311–313. (e) Liang, N. Ph.D. Dissertation, Northwestern University, 1988.

(4) The decay of  $\text{A}^*$  was followed both by  ${}^3\text{ZnP}$  emission and by  ${}^3\text{ZnP}$  transient absorption at  $\lambda = 475$  nm. Differences in  $k_p$  for the two Cc represent differences in both the rate constants for quenching by the ferriheme and in affinity constants.